

This article was downloaded by:

On: 25 January 2011

Access details: *Access Details: Free Access*

Publisher *Taylor & Francis*

Informa Ltd Registered in England and Wales Registered Number: 1072954 Registered office: Mortimer House, 37-41 Mortimer Street, London W1T 3JH, UK



## Separation Science and Technology

Publication details, including instructions for authors and subscription information:

<http://www.informaworld.com/smpp/title~content=t713708471>

### Membrane Electrode Assemblies Based on HYFLON® Ion for an Evolving Fuel Cell Technology

L. Merlo<sup>a</sup>; A. Ghielmi<sup>a</sup>; L. Cirillo<sup>a</sup>; M. Gebert<sup>a</sup>; V. Arcella<sup>a</sup>

<sup>a</sup> Solvay Solexis S.p.A., Bollate, MI, Italy

**To cite this Article** Merlo, L. , Ghielmi, A. , Cirillo, L. , Gebert, M. and Arcella, V.(2007) 'Membrane Electrode Assemblies Based on HYFLON® Ion for an Evolving Fuel Cell Technology', *Separation Science and Technology*, 42: 13, 2891 — 2908

**To link to this Article:** DOI: 10.1080/01496390701558334

URL: <http://dx.doi.org/10.1080/01496390701558334>

## PLEASE SCROLL DOWN FOR ARTICLE

Full terms and conditions of use: <http://www.informaworld.com/terms-and-conditions-of-access.pdf>

This article may be used for research, teaching and private study purposes. Any substantial or systematic reproduction, re-distribution, re-selling, loan or sub-licensing, systematic supply or distribution in any form to anyone is expressly forbidden.

The publisher does not give any warranty express or implied or make any representation that the contents will be complete or accurate or up to date. The accuracy of any instructions, formulae and drug doses should be independently verified with primary sources. The publisher shall not be liable for any loss, actions, claims, proceedings, demand or costs or damages whatsoever or howsoever caused arising directly or indirectly in connection with or arising out of the use of this material.



## Membrane Electrode Assemblies Based on HYFLON® Ion for an Evolving Fuel Cell Technology

**L. Merlo, A. Ghielmi, L. Cirillo, M. Gebert, and V. Arcella**

Solvay Solexis S.p.A., Bollate (MI), Italy

**Abstract:** The work presents an overview of the main properties of Hyflon® Ion perfluorosulfonic acid (PFSA) membranes for fuel cells in comparison with Nafion® PSFA membrane. The fuel cell performance of Hyflon® Ion-based membrane electrode assemblies (MEAs) is reported at medium (75°C) and high (120°C) temperature, demonstrating extremely good power output. Remarkable durability (5000 h) of the Hyflon® Ion product is also demonstrated in high power output conditions. The conductivity and the hydrogen permeability of Hyflon® Ion extruded membranes is reported in sub-freezing conditions (down to –40°C).

The degradation of the short-side-chain ionomer is investigated utilizing both ex-situ (Fenton) tests and fuel cell open circuit voltage tests. In the latter, the influence of the operating temperature on Hyflon® Ion degradation is not detectable in the range analysed (70°C–90°C). A better resistance to degradation of chemically stable Hyflon® Ion membranes (“S”-grades) vs. standard membranes results from all tests.

**Keywords:** Fuel cell, membrane, degradation, Hyflon® Ion, Dow ionomer

### INTRODUCTION

#### Long- and Short-Side-Chain Perfluorinated Ionomer Membranes

Perfluorosulfonic acid (PFSA) ionomers are known since the late 60s, when the Nafion® ionomers were developed by the DuPont company and

Received 15 January 2007, Accepted 21 May 2007

Address correspondence to V. Arcella, Solvay Solexis S.p.A., 20021 Bollate, (MI), Italy. Tel.: + 39 02 3835 6527; Fax: +39 02 3835 6355; E-mail: vincenzo.arcella@solvay.com

employed as polymer electrolyte in a GE fuel cell designed for NASA spacecraft missions. Since then, Nafion® polymers have found wide application especially in the chlor-alkali industry as membrane materials, but also in other applications where very high chemical inertness (given by the perfluorinated structure) and low resistances to cation transport are required at the same time.

In more recent years, the growing interest related to cleaner energy production technologies has promoted the consideration and study of ionomers as proton-exchange membranes (PEMs) in fuel cells. Again, due to electrochemical stability requirements, perfluorinated materials have been preferred as the best candidates for satisfying the needs of the system.

In the mid 1980s Ballard Power Systems showed significant improvements in fuel cell performance using ionomer membranes obtained from Dow Chemical (1). This ionomer, commonly known as the Dow ionomer, is perfluorinated and similar in structure to Nafion®, save for a shorter pendant side-chain which carries the functional ion-transporting group, wherefrom this ionomer is known as the short-side-chain (SSC) ionomer. Correspondingly, Nafion® is sometimes referred to as the long-side-chain (LSC) ionomer. Though demonstration of a higher power-generating capability in fuel cell was given using the Dow ionomer, after the filing of a series of patents by the Dow company (2–10), the industrial development of this interesting ionomer structure was abandoned. The complexity of the Dow process for the synthesis of the base functional monomer used for the production of the SSC ionomer (11) was possibly one of the reasons which caused this interesting development to be abandoned.

Recently, due to a different and simpler route for the synthesis of the base monomer for SSC ionomers (11), Solvay Solexis has restarted the development of polymer electrolyte membranes based on this perfluorinated ionomer type. The commercial name for this ionomer (and the membranes made there from) is Hyflon® Ion. Figure 1 illustrates the chemical structure of different PFSA polymers reported in the literature and available on the

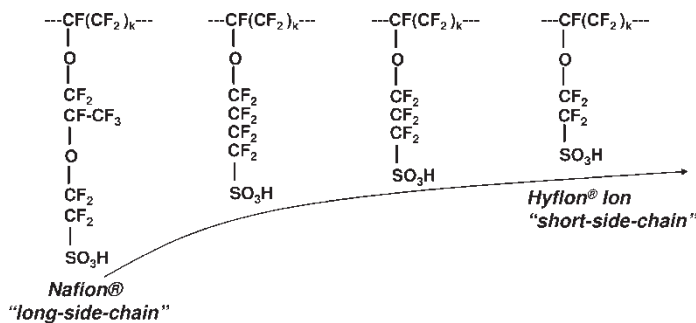


Figure 1. Different PFSA polymers reported structures.

market, showing Hyflon® Ion as the one possessing the shortest side chain among all.

### SSC Ionomers: Polymer and Membranes Properties

The works by Tant et al. (12, 13) and by Moore and Martin (14) contain very significant data on SSC ionomers of different equivalent weights (EWs) and highlight important differences induced by the shorter length of the side chain compared to a LSC ionomer. In particular, crystallinity—measured by wide-angle X-ray scattering (WAXS) and differential scanning calorimetry (DSC)—and dynamic-mechanical properties—investigated by dynamic mechanical spectroscopy (DMS)—are studied for all forms of existence of the ionomer during the synthesis process, i.e., the precursor ( $\text{SO}_2\text{F}$ ), salt ( $\text{SO}_3\text{Na}$ ), and acid ( $\text{SO}_3\text{H}$ ) form. The most significant differences found are the much higher crystallinity at given equivalent weight of the SSC ionomer compared to the LSC one and the higher glass transition temperature ( $T_g$ ) of the SSC ionomer. This is true for all ionomer forms examined. Extrapolation of both WAXS and DSC data on different EW precursor polymers show disappearance of crystallinity below 700 EW for the SSC ionomer, compared to 965 EW for Nafion®. This allows for a wider operating window towards lower EW ionomers still retaining good mechanical properties and substantial water insolubility.

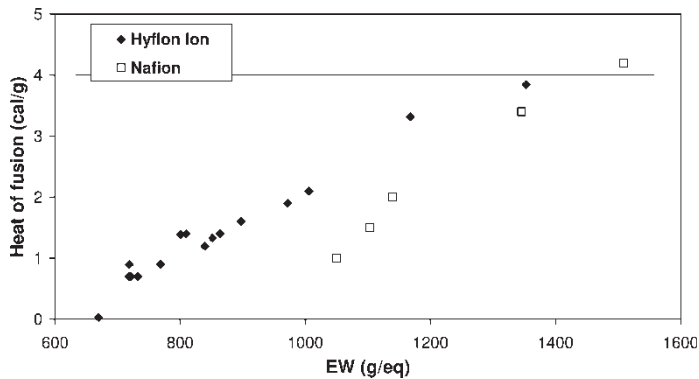
Data on Hyflon® Ion membranes, including fuel cell performance, mechanical characteristics and hydration properties were published in (15, 16) and resulted in most cases comparable to the data published on the Dow ionomer, a few important topics are listed below.

Figure 2 reports the difference in crystallinity level between Hyflon® Ion and Nafion® ionomers as a function of the EW (ionomer precursor, i.e.,  $\text{SO}_2\text{F}$ , forms). The higher crystallinity of Hyflon® Ion at any fixed EW is a consequence of its shorter side chain, allowing an easier chain packing into the backbone of the chain (crystallisable macromolecule portion).

Figure 3 reports the temperature of complete fusion of the SSC polymer (precursor form) as a function of the EW, experimental data are compared with literature data described for Dow Ionomer. A good correlation can be found between the two and a linear increase of the temperature of complete fusion from the equivalent weight is evidenced.

Figures 4 and 5 report the Dynamic Mechanical Spectroscopy (DMS) analysis of Hyflon® Ion and Nafion® membranes, showing the higher glass transition temperature of Hyflon® Ion.

Finally, Figure 6 reports the membrane hydration at 100°C (water soaking), again a good correspondence between experimental data on Hyflon® Ion and literature data from Dow ionomer is reported (the latter much more scattered).



**Figure 2.** Heats of second fusion of Hyflon<sup>®</sup> Ion precursor polymers vs. Nafion<sup>®</sup> as a function of EW.

The Hyflon<sup>®</sup> Ion membranes used in the experimental part of this work have an EW in the range of 850–870 g/eq. This EW range guarantees good mechanical properties due to the high crystallinity level and a hydration level high enough to give high proton conductivity. The values of crystallinity and hydration for this EW range can be derived from the figures described above. Results on chemically stable Hyflon<sup>®</sup> Ion membranes (“S”-grade) in the same EW range are also reported in this work. These membranes are especially designed in order to resist to the degradation reaction mechanisms which are discussed in the following section without having significant modification, compared with standard grades, regarding mechanical resistance and fuel cell performances (polarization curve).

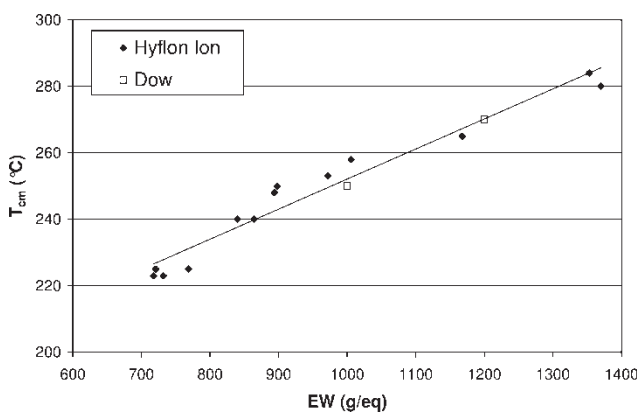


**Figure 3.** Temperature of complete fusion of SSC precursor polymers as a function of EW.

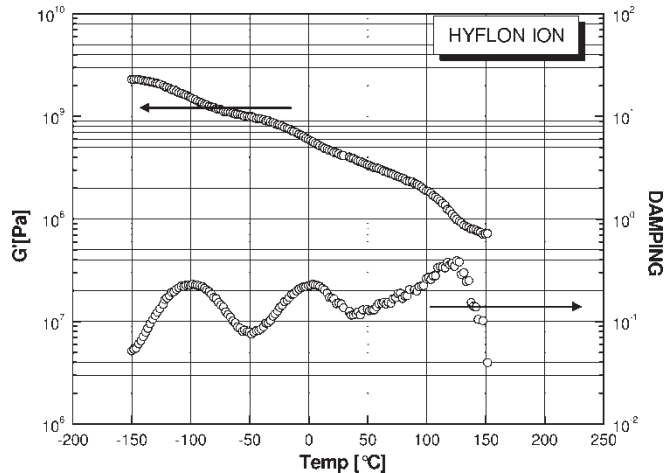


**Figure 4.** Dynamic mechanical spectrum of an 850 EW Hyflon® Ion acid form membrane (pre-dried at 150°C under vacuum).

### Membrane Peroxide Degradation: State of the Art

Among the mechanisms reported in the literature which describe the degradation of PFSA membranes, the one generally recognized as the most relevant by the scientific community is the so called “unzipping reaction” originated by peroxide radical attack. This is described, for example, by Curtin et al. (17).

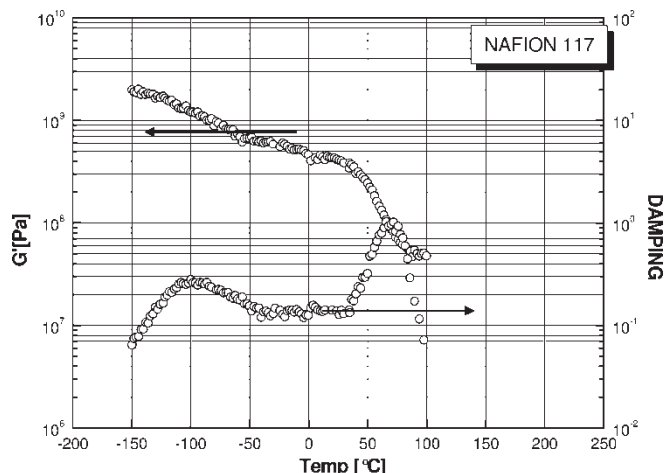


**Figure 5.** Dynamic mechanical spectrum of an 1100 EW Nafion® acid form membrane N117 (pre-dried at 150°C under vacuum).

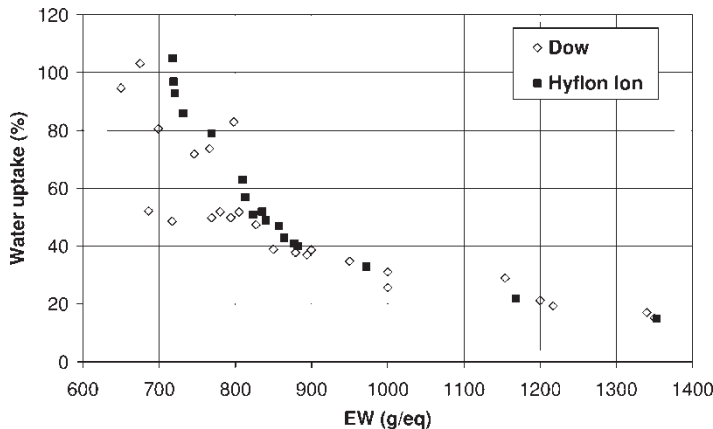
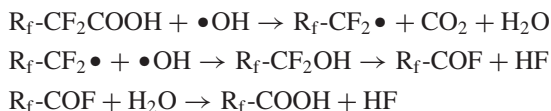


**Figure 6.** Water uptake from liquid water at 100°C for extruded Hyflon® Ion and Dow membranes as a function of equivalent weight.

The “unzipping reaction” process starts from the carboxylic end groups present in the polymer as a consequence of the polymerization process and disgregates the main chain of the polymer according to the following reaction scheme:



During this process evolution of  $\text{CO}_2$  and HF can be detected. In fact the preferred methods for checking the degradation level are:

1. The weight reduction of the polymer (18)
2. The measure (via selective electrodes or ionic chromatography) of the F-ions released (19–24)
3. Measure of the pH reached by the solution (22) (in direct relation with the amount of F-due to the low acid force of HF,  $K_a = 6.7\text{E-}4$ ). This last should be considered carefully because of the possible presence in solution of  $R_f\text{-SO}_3\text{H}$  residuals that reduce further the pH level.

It is generally recognized that the degradation mainly occurs due to the presence of the  $\bullet\text{OH}$  species that is guaranteed by the decomposition of  $\text{H}_2\text{O}_2$ . The  $\text{H}_2\text{O}_2$  is present preferentially on the anode side, where the potential is low enough, and is formed as a consequence of oxygen crossover (25) through the membrane. Hydrogen peroxide had been detected in both anode and cathode condenses in a concentration directly proportional to the membrane gas crossover level (26). Other factors that can

influence and increase the presence of hydrogen peroxide in a working fuel cell are the type of catalyst and the presence of chlorine ions in the catalyst (27) as well. The latter are residuals from noble metal precursors in some catalyst productions.

The decomposition of  $\text{H}_2\text{O}_2$  to give the peroxide radical species is definitely increased by the presence of traces of metal ions such as iron (22), copper (28), or titanium (29), but the degradation of PFSA membranes is described even in the absence of these pollutants (18, 24).

Tests based on Fenton reagents (17, 29, 30) are often used to simulate peroxide attack to PFSA membranes before carrying out long-term fuel cell tests. However, a shared Fenton test protocol is not yet defined. The main reaction occurring in the Fenton medium is:



The peroxide degradation rate of PFSA membranes is recognized to be directly related to the amount of carboxylic (-COOH) end groups present in the polymer. This is proven by studies on model compounds (23, 31) and from the direct testing of membranes realized with a reduced content of end groups. These products are usually presented as "stabilized" (17, 31, 32).

Regarding fuel cell testing, high voltage conditions are agreed to be the preferred conditions for highlighting membrane tendency to degradation (33).

## EXPERIMENTAL

### Membrane Preparation

Ionomer precursor polymers were obtained by semi-batch emulsion copolymerization of the perfluorinated short-side-chain sulfonyl-fluoride-vinyl-ether (SSC-SFVE) of formula  $\text{CF}_2=\text{CF}_2-\text{O}-\text{CF}_2-\text{CF}_2-\text{SO}_2\text{F}$  (perfluoro-5-sulfonyl-fluoride-3-oxa-1-pentene) with tetrafluoroethylene (TFE) in an autoclave by using fixed TFE pressures and SSC-SFVE feed rates in order to obtain the desired EW.

The polymer was recovered by freeze-thawing the latex, washed with demineralized water, and oven dried above 100°C. The polymer was then pelletized and melt-extruded into a film of the desired thickness in a screw extruder at a temperature at least 30°C above the complete melting of the polymer as determined by DSC.

The film thus obtained was converted into the salt form by immersion in a KOH/water 10/90 w/w solution at 80°C for a time long enough to detect complete disappearance of the  $\text{SO}_2\text{F}$  groups by IR analysis (transmission). The film was then washed and acidified twice in an excess

amount of  $\text{HNO}_3$ . The resulting membrane was finally washed in demineralized water.

### Ionomer Dispersion Preparation

Ionomer precursor polymers obtained as described above were synthesized, recovered from the latex, washed and dried. The obtained polymer powder was then hydrolysed converting it to the salt form by immersion in a KOH/water 10/90 w/w solution at 80°C for a time long enough to detect complete disappearance of the  $\text{SO}_2\text{F}$  groups and then acidified in an excess amount of  $\text{HNO}_3$ . The polymer powder was then washed and dried.

The polymer dispersion was then obtained by dissolving the polymer powder in an autoclave by a high temperature process similar to what described by Grot in (34).

### Membrane Electrode Assembly Preparation and Cell Assembly

The testing apparatus consists in 25  $\text{cm}^2$  single cells (Fuel Cell Technologies<sup>®</sup>) with triple serpentine pattern flow fields, mounted on Arbin<sup>®</sup> 50 W test stations.

The Hyflon<sup>®</sup> Ion membranes thickness was 50 micron and the equivalent weight 870 g/eq. The electrodes were fabricated on a PTFE support by casting hydro-alcoholic inks produced from ionomer dispersion of EW = 830 g/eq and a commercial Pt/C 50% by weight on Vulcan XC-72. The casting blade height was adjusted in order to have a Pt load of 0.25 mg/ $\text{cm}^2$  of platinum on both anode and cathode electrodes. The two electrodes were transferred by high temperature “decal” onto the membrane; the cells were assembled using two commercial carbon felt gas diffusion layers 0.4 mm thick, with a thin “micro-diffusion layer” on one side. The gas diffusion layers were assembled with the micro-diffusion layers facing the electrodes. The cells were closed with a torque of 5 Nm on each of the 8 tie rods. Rigid gaskets 0.26 mm thick were present on both anode and cathode side. The MEAs were protected with a thin, rigid subgasket on both sides before assembly; the active area was reduced to 20  $\text{cm}^2$  by the presence of the subgasket.

Before starting each test, the MEAs were conditioned for 8 hours in the following operating conditions:

Fixed current: 1000 mA/ $\text{cm}^2$

Cell temperature: 75°C

Air flow: 1300 sccm (2.5 bara, dew point 80°C)

Hydrogen flow: 650 sccm (2.5 bara, dew point 80°C)

### Fenton Test Procedure

The following Fenton test conditions were adopted:

Iron salt:  $\text{Fe}(\text{NH}_4)_2(\text{SO}_4)_2$

Iron concentration: 36 ppm of  $\text{Fe}^{2+}$  in solution

Hydrogen peroxide concentration: 15 or 30% by volume

Bath temperature: 55°C

Reaction time (without inserting fresh  $\text{H}_2\text{O}_2$ ): 6 hours

Membrane sample weight: 1 gram

The reagents are mixed at ambient temperature by correcting the pH of the  $\text{Fe}^{2+}$  solution with  $\text{H}_2\text{SO}_4$  in order to reach a pH level below 3 before the addition of  $\text{H}_2\text{O}_2$ . The membrane sample is then added and the solution is heated to 55°C. The 6 hours of reaction are considered to start when the set temperature of 55°C is reached.

The fluoride level is measured with an Ion Selective Electrode Ionplus 9009BN after the removal of the non-reacted  $\text{H}_2\text{O}_2$  and the addition of a buffer solution (TISAB III).

## RESULTS AND DISCUSSION

### Fuel Cell Performance Verification

After the conditioning of the electrochemical package (i.e., MEA) a first characterization of performance was implemented at medium temperature in the following operating conditions with air:

Cell temperature: 75°C

Hydrogen flow: 650 sccm (2.5 bara, dew point 80°C)

Air flow: 1300 sccm (2.5 bara, dew point 80°C)

and with pure oxygen:

Oxygen flow: 800 sccm (2.5 bara, dew point 80°C)

In a similar way the performance in a high temperature condition was recorded:

Cell temperature: 120°C

Air flow: 1300 sccm (2.5 bara)

The polarization curves and the corresponding power density curves of these three tests are shown in Figs. 7, 8 and 9, respectively. It should be noted that

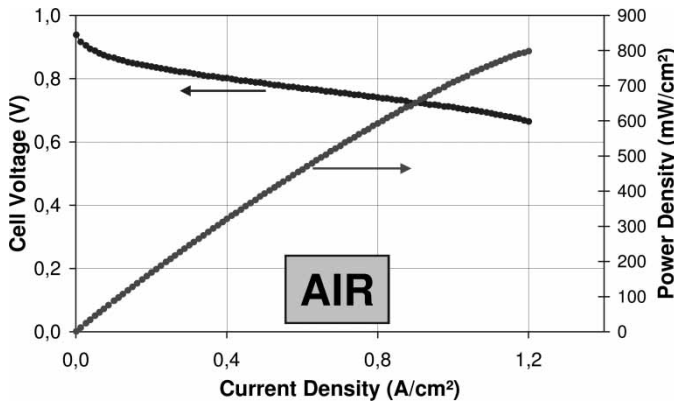


**Figure 7.** Polarization and power curves of a Hyflon® Ion MEA at medium temperature (75°C) in air. Saturated reactants at 2.5 bara.

the Hyflon® Ion-based MEA is able to maintain a voltage of 0.75 V at a current density of 0.8 A/cm<sup>2</sup> both at 75°C and 120°C with air.

#### Fuel Cell Durability Test in Steady State Operation at Medium Temperature

Using the same operating conditions detailed above for the test of Fig. 7, a durability test was started by fixing the cell voltage to 0.6 V (corresponding to an average current density during the test of 1.05 A/cm<sup>2</sup>).

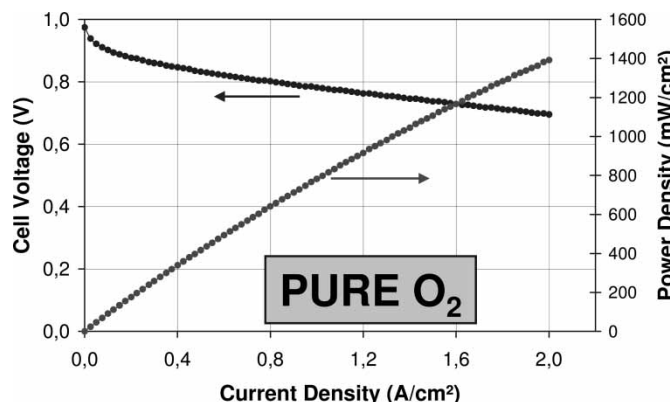


**Figure 8.** Polarization and power curves of a Hyflon® Ion MEA at medium temperature (75°C) in pure oxygen. Saturated reactants at 2.5 bara.

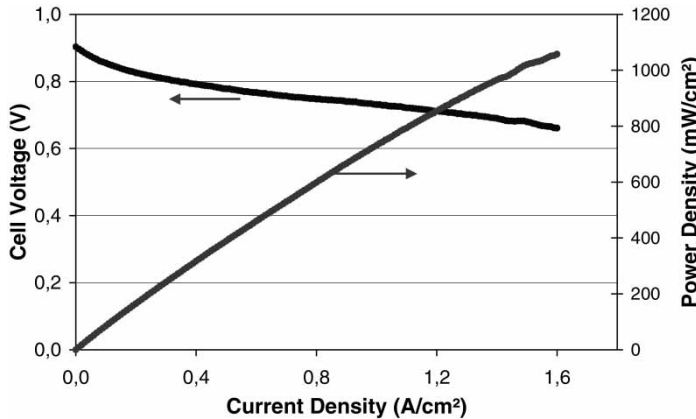


**Figure 9.** Polarization and power curves of a Hyflon® Ion MEA at high temperature (120°C) in air. Saturated reactants at 2.5 bara.

The test lasts 5000 hours in steady state, while recording a polarization curve every 100 hours of test and checking periodically the membrane gas crossover. At the end of the test, as it can be observed from Fig. 10, the electrochemical package degradation is very limited and concentrated in the diffusion part of the polarization curves (loss of gas diffusion layer's hydrophobic properties), while the portion of the curve related to membrane and electrode performance is virtually unaffected. Actually, hydrogen crossover measures confirmed no formation of pinholes or even membrane thinning.

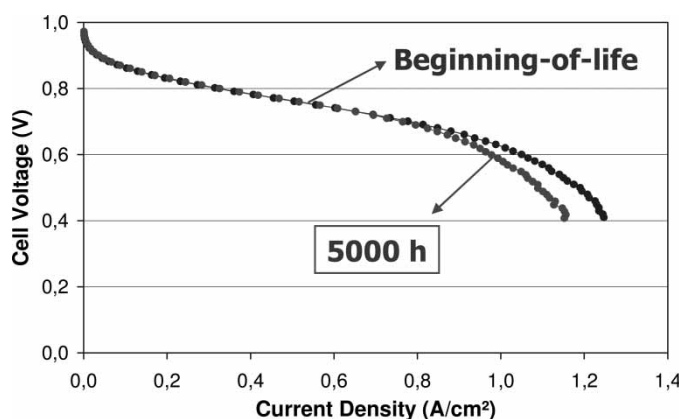


**Figure 10.** Polarization curves at hour zero and hour 5000 for a Hyflon® Ion MEA tested at medium temperature (75°C) in air, with saturated reactants at 2.5 bara, and at a constant potential of 0.6 V.

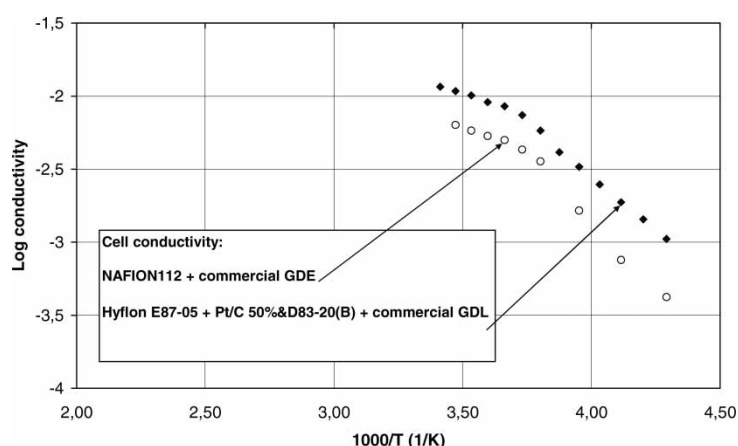
### Fuel Cell Membrane Behavior in Freezing Conditions

One of the most important properties that a PFSA membrane must guarantee in automotive application, for ensuring winter vehicle start, is a limited increase in resistivity at very low temperatures.

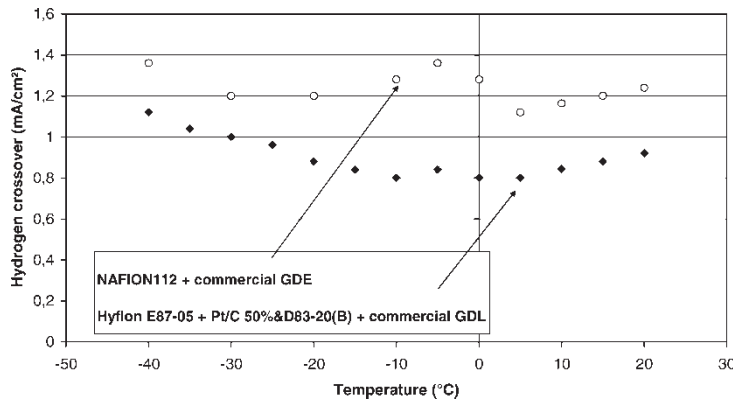
By maintaining the fuel cell at controlled temperatures (starting from  $-40^{\circ}\text{C}$ ) the conductivity of the membrane was measured together with the hydrogen crossover current. The electrochemical characterization was implemented with a PGSTAT30 equipped with FRA2 and with a 20 A current elevator from ECO-CHEMIE.

Figure 11 shows the cell conductivity (in form of Arrhenius plot) of a Hyflon<sup>®</sup> Ion membrane compared with a Nafion<sup>®</sup> N112 membrane. It can be observed that Hyflon<sup>®</sup> Ion shows higher conductivity values with a fairly constant difference throughout the whole low-temperature interval. These data add on to the higher conductivity values already reported for Hyflon<sup>®</sup> Ion at  $35^{\circ}\text{C}$  over a broad relative humidity range (35). In Fig. 11 it is interestingly observed that a change in the slope of the conductivity curve occurs around the water freezing point. This highlights a change in the activation energy of the proton transport mechanism. The temperature at which this occurs appears to be similar for Nafion<sup>®</sup> and Hyflon<sup>®</sup> Ion.

Figure 12 shows the membrane hydrogen crossover as a function of temperature over the same temperature range. Independently from temperature, Hyflon<sup>®</sup> Ion shows lower hydrogen permeability compared to N112.



**Figure 11.** Hyflon<sup>®</sup> Ion MEA conductivity as a function of temperature down to  $-40^{\circ}\text{C}$  in comparison with Nafion<sup>®</sup>.



**Figure 12.** Hyflon® Ion MEA hydrogen crossover current as a function of temperature down to  $-40^{\circ}\text{C}$  in comparison with Nafion®.

### Fuel cell Open Circuit Voltage Test Results

A test campaign was performed in order to verify membrane degradation in different operating conditions, particularly temperature and reactants humidification, during OCV tests. Four cells with the same electrochemical package were tested, with different temperature and reactant humidification:

1. Cell temperature:  $70^{\circ}\text{C}$ , reactants humidification 100%
2. Cell temperature:  $70^{\circ}\text{C}$ , reactants humidification 50%
3. Cell temperature:  $90^{\circ}\text{C}$ , reactants humidification 100%
4. Cell temperature:  $90^{\circ}\text{C}$ , reactants humidification 50%

All the other operating conditions were exactly the same for all the 4 tests:

Cell current density:  $0 \text{ mA/cm}^2$

Air flow:  $500 \text{ sccm}$  (outlet pressure 1.5 bara) Compressed air  
( $1 \mu\text{m}$  filter applied)

Hydrogen flow:  $500 \text{ sccm}$  (inlet pressure 1.5 bara) Pure hydrogen  
(5.5 grade)

The membrane degradation, monitored through the hydrogen crossover increase, is detailed in Fig. 13. It can be observed that there is a clear increase in the degradation rate when there is a reduction of reactants humidification, while the different operating temperature does not influence the degradation rate. This indicates that, in the absence of a different degradation origin, high temperature operation itself does not represent a condition of reduced lifetime for Hyflon® Ion membranes. The high glass transition

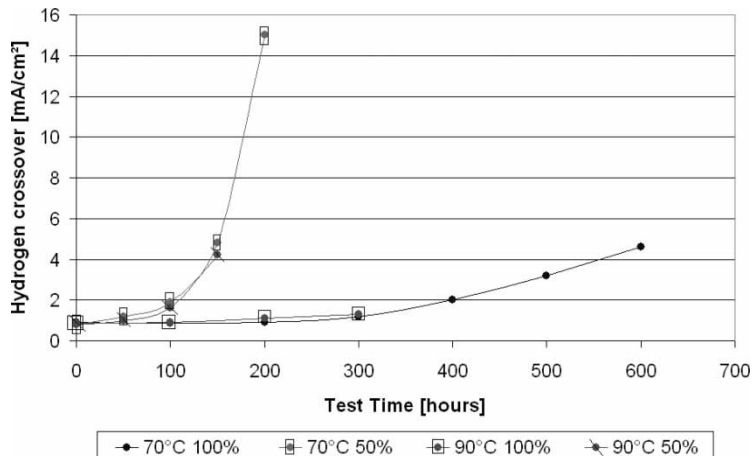


**Figure 13.** Comparison of hydrogen crossover current density ( $\text{mA cm}^{-2}$ ) in time for Hyflon® Ion extruded membranes in OCV tests with different operating temperature and reactants humidification.

temperature of the Hyflon® Ion polymer (see Fig. 4) guarantees that mechanical degradation phenomena (creep) do not occur at a temperature level around 90°C and above.

Another test campaign was carried out in order to test the stabilized (“S”-grade) Hyflon® Ion polymer in OCV tests.

As shown in Fig. 14 both at 70°C/100% humidification and at 90°C/50% humidification there is a higher resistance to degradation of the stabilized extruded membrane compared with the standard one. The OCV durability of the stabilized membrane is increased by a factor of approximately 5X. The conductivity of the cell was monitored during all the tests and no increase was noticed at any time.

### Fenton Test Results

In order to confirm the difference in degradation behavior between standard and stabilised Hyflon® Ion and to compare it with other commercial PFSA membranes, an accelerated ex-situ degradation test (Fenton test) was implemented with the procedure previously described. The fluoride release value for the Hyflon® Ion extruded membrane (E87-05) is aligned to the value obtained on the Nafion® N112 membrane, the cast Nafion® membrane (NR112) showing a slightly lower value.

A substantially lower fluoride release is observed by testing a stabilized Hyflon® Ion membrane (E87-05S), as it can be observed in Fig. 15.

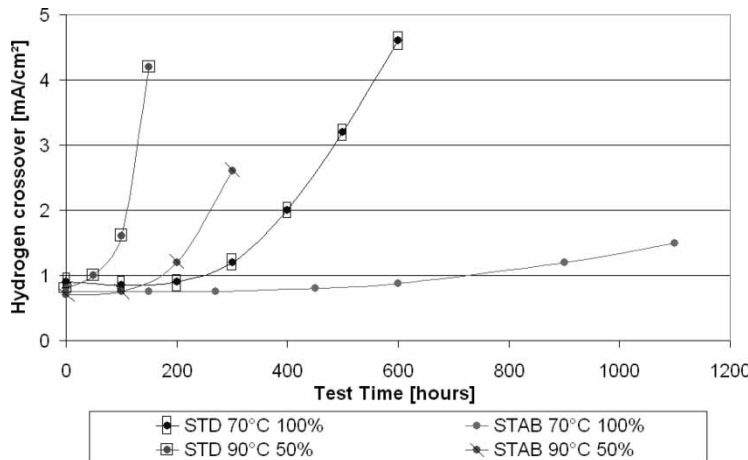


**Figure 14.** Comparison of hydrogen crossover current density ( $\text{mA cm}^{-2}$ ) in time for Hyflon<sup>®</sup> Ion standard extruded membranes and stabilized extruded membranes in OCV tests with different operating conditions.

In order to check the evolution in time of the degradation of the polymer when subject to peroxide radical attack, a second kind of test was carried out by extracting the membrane from the Fenton solution every 6 hours, purifying it by acid treatment and washing, and reinserting the membrane in fresh Fenton reagents. The fluoride amount in the different solutions obtained in

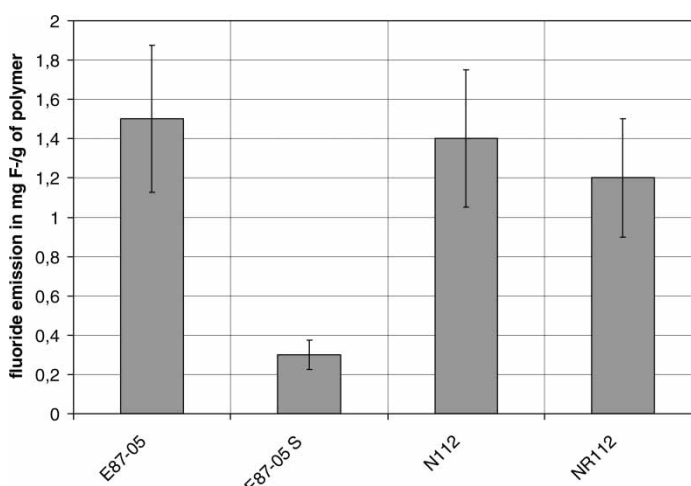


**Figure 15.** Fluoride emission (mg F-per gram of polymer) for standard extruded Hyflon<sup>®</sup> Ion (E87-05), stabilized extruded Hyflon<sup>®</sup> Ion (E87-05S), Nafion<sup>®</sup> N112 (extruded) and Nafion<sup>®</sup> NR112 (cast) membranes.

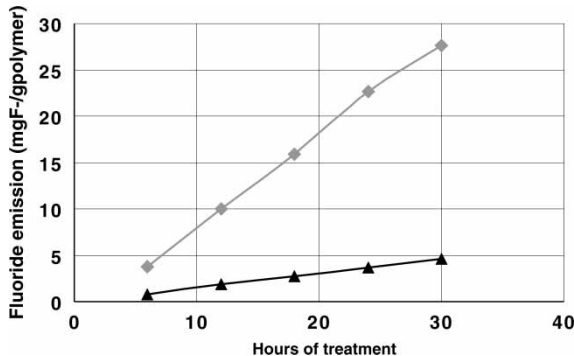


**Figure 16.** Cumulative fluoride emission (mg F-per gram of polymer) in prolonged Fenton tests for standard extruded Hyflon® Ion (squares) and stabilized extruded Hyflon® Ion (triangles) membranes.

this way was measured. The result of this test, shown in Fig. 16, is a linear increase of the cumulative fluoride emissions with time for both standard and stabilized grades. The difference in degradation rate between the standard and the stabilized Hyflon® Ion is maintained in this prolonged test and there is no evidence of the reduction or increase of the degradation rate during time. This suggests that the number of chain sites which are attacked by the peroxide radicals remains constant in time. This is consistent with the “unzipping reaction” mechanism, where from a carboxylic end group another identical group is generated (no change in number).

## CONCLUSIONS

A review of the main properties of Hyflon® Ion membranes has been presented and a comparison with Nafion® PSFA membrane reported.

The fuel cell performance of Hyflon® Ion-based membrane electrode assemblies (MEAs), at medium (75°C) and high (120°C) temperature were measured, both in air and pure oxygen, with extremely good power output. Remarkable durability of the Hyflon® Ion product was also demonstrated. The conductivity and the hydrogen permeability of Hyflon® Ion extruded membranes were measured down to -40°C, with constantly better behaviour compared to Nafion®.

The degradation of the short-side-chain ionomer was investigated utilizing both ex-situ (Fenton) tests and in-situ (fuel cell) tests. The peroxide degradation mechanism was highlighted in open circuit voltage (OCV) tests at different operating temperatures and reactants humidification. The influence of the operating temperature on Hyflon® Ion degradation is not detectable in the range analyzed (70°C–90°C) while there is a quite important influence of the humidification level.

Long term Fenton tests delivered a linear behavior of membrane degradation, which is consistent with the “unzipping reaction” from chain-end groups being the dominant degradation mechanism in the range of concentrations analysed. The higher stability of stabilized Hyflon® Ion membranes (“S”-grades) vs. standard membranes has been shown in all tests, both single cell OCV tests and Fenton tests (normal and prolonged).

## ACKNOWLEDGEMENTS

Many thanks to all the Solvay Solexis personnel involved in ionomer synthesis, membrane preparation, ex-situ characterization and fuel cell testing, whose contribution has determined the generation of the products and data which are the subject of the present work.

## REFERENCES

1. Prater, K. (1990) *J. Power Sources*, 29: 239–250.
2. Ezzell, B.R., Carl, W.P., and Mod, W.A. USP 4,330,654, 1982.
3. Ezzell, B.R., Carl, W.P., and Mod, W.A. USP 4,358,545, 1982.
4. Ezzell, B.R., Carl, W.P., and Mod, W.A. USP 4,417,969, 1983.
5. Ezzell, B.R., Carl, W.P., and Mod, W.A. USP 4,470,889, 1984.
6. Ezzell, B.R., Carl, W.P., and Mod, W.A. USP 4,478,695, 1984.
7. Ezzell, B.R., Carl, W.P., and Mod, W.A. USP 4,834,922, 1989.
8. Ezzell, B.R. and Carl, W.P. USP 4,940,525, 1990.
9. Carl, W.P., Cisar, A.J., Door, R.D., and Black, L.L. EP application 0 498 076 A1, 1992.
10. Alexander, L.E. and Eisman, G.A. EP specification 0 221 178 B1, 1993.
11. Arcella, V., Ghielmi, A., and Tommasi, G. (2003) *Ann. N.Y. Acad. Sci.*, 984: 226–244.
12. Tant, M.R., Darst, K.P., Lee, K.D., and Martin, C.W. (1989) Multiphase polymers: blends and ionomers. In: Utracki, L.A. and Weiss, R.A. (eds.); ACS: Washington, 370–400, ACS Symp. Ser. 395.
13. Tant, M.R., Lee, K.D., Darst, K.P., and Martin, C.W. (1988) *Polym. Mat. Sci. Eng.*, 58: 1074–1078.
14. Moore, R.B. and Martin, C.R. (1989) *Macromolecules*, 22: 3594–3599; Eisman, G.A. (1986) Proceedings of the 168th Electrochemical Society Meeting, 83–13, 156–171.
15. Ghielmi, A., Vaccarono, P., Troglia, C., and Arcella, V. (2005) *Journal of Power Sources*, 145 (2): 108–115.
16. Arcella, V., Troglia, C., and Ghielmi, A. (2005) *Industrial & Engineering Chemistry Research*, 44: 7646–7651.
17. Curtin, D.E., Lousenberg, R.D., Henry, T.J., Tangeman, P.C., and Tisack, M.E. (2004) *Journal of Power Sources*, 131 (1–2): 41–48.
18. Hommura, S., Kawahara, K., and Shimohira, T. Degradation Mechanism of Perfluorinated Membrane in Fuel Cell Environment, Fuel cell Seminar 2005 Abstracts.
19. Liu, W., Ruth, K., and Rusch, G. (2001) *Journal of New Materials for Electrochemical Systems*, 4: 227–231.

20. Mittal, V., Kunz, H.R., and Fenton, J.M. Factors Accelerating Membrane Degradation Rate and the Underlying Degradation Mechanism in PEMFC, 208th Meeting of the Electrochemical Society proceedings.
21. Los Alamos National Labs, Durability Issues of the PEMFC GDL and MEA under Steady-state and Drive-cycle Operating conditions, Fuel Cell Seminar 2005 Abstracts.
22. Pozio, A., Silva, R.F., De Francesco, M., and Giorgi, L. (2003) *Electrochimica Acta*, 48: 1543–1549.
23. Hicks, M.T. DOE Hydrogen program report. Contract N° DE-FC36-03GO13098.
24. Aoki, M., Uchida, H., and Watanabe, M. (2005) *Electrochemistry Communication*, 7: 1434–1438.
25. The 4th International Conference on Application of Conducting Polymer proceedings; Doshisha University.
26. Liu, W. and Zuckebrod, D. (2005) *Journal of the Electrochemical Society*, 152 (6): A1165–A1170.
27. Schmidt, T.J., Paulus, U.A., Gasteiger, H.A., and Behm, R.J. (2001) *Journal of Electroanalytical Chemistry*, 508 (1–2): 41–47.
28. Kadirov, M.K., Bosnjakovic, A., and Schlick, S. (2005) *J. Phys. Chem. B*, 109 (16): 7664–7670.
29. Bosnjakovic, A. and Schlick, S. (2004) *J. Phys. Chem. B*, 108: 4332–4337.
30. Namkung, K.C. and Sharratt, P. Fenton and Photo-Fenton Processes for Treatment of Aqueous Wastes, UMIST.
31. Escobedo, G. Strategies to Improve Durability of Perfluorosulfonic Acid Membranes for PEMFC, FC Durability 2005 Proceedings.
32. Anderson, E. Improved Membrane Durability in Water Electrolyzers, FC Durability 2005 Proceedings.
33. Qi, Z. FC Durability for Stationary Applications: From Single Cells to Systems, FC Durability 2005 Proceedings.
34. Grot, W.G. USP 4,433,082, 1984.
35. Ghielmi, A., Meunier, V., Merlo, L., and Arcella, V. (2005) *Prepr. Pap.-Am. Chem. Soc., Div. Fuel Chem.*, 50 (2): 521.